Propagating lattice instabilities in shock-loaded metals

Paul A. Taylor and Brian W. Dodson
Sandia National Laboratories, Albuquerque, New Mexico 87185
(Received 1 February 1990)

The first atomic-scale simulations of shock propagation using accurate many-body atomic interactions have been performed. Shock propagation in copper was modeled with use of the embedded-atom method. Lattice instabilities, consisting of crystallographic twinning boundaries and martensitic regions, were observed to form and propagate behind the shock front for impact velocities as low as 0.01 km/sec. The twinning boundary dislocations cause a loss of shear strength, resulting in a significant reduction in shock-wave velocity, without the accompaniment of permanent crystallographic damage. This new mode of lattice deformation is qualitatively different from the behavior characteristic of pairwise atomic interactions.

INTRODUCTION

A shock wave is generated in a solid by high-velocity impact. Shock loading of metals at moderate velocities (perhaps 0.2–0.4 km/sec) produces a wide range of nonequilibrium effects, such as dynamic mixing and shear band nucleation. In a perfect single crystal, these effects are thought to be initiated by mechanisms taking place on a size scale of a few nanometers. In real samples, however, interaction with defect structures broadens the observed shock-wave profiles to widths of 10–100 μm. Current experimental diagnostics have spatial resolution limits on a similar scale. The microscopic mechanisms underlying many important shock-loading effects are thus not currently accessible to experimental study.

Molecular dynamics simulations using pairwise atomic interactions have previously been performed to study shock loading in perfect crystals.[1–4] Although various regimes of material response (i.e., elastic, elastic-plastic, and plastic) to shock loading have been observed,[4] these simulations have not predicted the existence of structural changes where nonequilibrium effects have been observed experimentally.

We have carried out what we believe to be the first molecular dynamics simulations of shock propagation, taking into account many-body interactions, in initially perfect single crystals of copper. The atomic interactions are modeled using the embedded-atom method.[5] Identical simulations using a pairwise potential are performed as well in an attempt to distinguish the many-body effects in the shock process. A new and significant result of this work is the prediction of the formation of lattice instabilities, consisting of twinning boundaries and martensitic regions, which propagate behind the shock front at low to moderate shock strengths (<20 GPa). The net effect of these propagating instabilities is a substantial reduction in shear strength without the accompaniment of permanent crystallographic damage.

ATOMISTIC SIMULATION OF SHOCK PHENOMENA

The many-body atomic interactions are modeled using the embedded-atom method, where the total cohesive energy is approximated by the form

$$E_{\rm coh}=\sum_i F_i(\rho_{h,i})+\tfrac{1}{2}\sum_{\substack{i,j\\ j\neq i}}\phi(R_{ij})\ . \tag{1}$$

In this expression, $\rho_{h,i}$ is the host electron density at atom i due to the remaining atoms of the system. $F_i(\rho)$ is the energy to embed atom i into the background electron density ρ, and $\phi(R_{ij})$ is the core-core pair repulsion between atoms i and j separated by the distance R_{ij}. The electron density is approximated by the superposition of atomic electron densities through

$$\rho_{h,i}=\sum_{j\ (\neq i)}\rho_j^a(R_{ij})\ , \tag{2}$$

where ρ_j^a is the electron density contributed by atom j. In this representation the embedding functions F_i account for the many-body interactions, whereas the function ϕ models pair interactions of a Coulombic nature. To apply this method, the embedding functions F_i, pair repulsion ϕ, and atomic densities ρ_j^a must be known. These quantities are empirically determined by fitting to the sublimation energy, equilibrium lattice constant, elastic constants, and vacancy-formation energies of the metal in question. This fitting procedure has been outlined in detail by Foiles *et al.*,[5] with the resulting parameters for copper taken from that reference for use in the present work.

The pairwise simulations use a Morse-type potential and are performed under identical conditions as those using the embedded-atom method. The choice of this potential is based on the work of Abell,[6] who has shown that the bonding can be properly described by pairwise interactions (for which a Morse-type potential is a reasonable approximation), but the strength of the pairwise interaction is influenced by the local environment, e.g., by many-body interference terms. In the pairwise simulations, the total cohesive energy is given by

$$E_{\rm coh}=\tfrac{1}{2}\sum_{\substack{i,j\\ j\neq i}}\Phi(R_{ij})\ , \tag{3}$$

with

$$\Phi(R)=D\{\exp[-2\beta(R-R_0)]-2\exp[-\beta(R-R_0)]\}\ , \tag{4}$$

where the parameters D, β, and R_0 are related to the binding energy E_b, bulk modulus B, and lattice constant a_0, at equilibrium, through

$$D=E_b/6\ ,$$
$$\beta=\left[\frac{9Ba_0}{4E_b}\right]^{1/2}\ , \tag{5}$$
$$R_0=a_0/\sqrt{2}\ .$$

The values of these material properties for copper are the same as those used in the fitting of the embedded-atom method potential, Eqs. (1) and (2)—namely $E_b=3.54$ eV, $B=1.38$ ergs/cm^3, and $a_0=3.615$ Å.

In the present work a shock wave is generated by colliding an atomic copper impactor with a nondeforming, stationary wall of copper on the ⟨001⟩ face. The fcc copper impactor is 4×4 unit cells (14.5×14.5 Å^2) perpendicular to the shock direction and either 30 or 60 atomic planes (52.4 or 106.6 Å) in length. The impactor is initially equilibrated at zero pressure and 300 K, permitting surface relaxation to occur. Periodic boundary conditions are imposed perpendicular to the shock direction; no size effects are found in studies of larger impactors. The particle velocity U_p of the desired shock state is superimposed upon the initial thermal motion of the impactor lattice. U_p was varied from 0.01 to 2.5 km/sec, corresponding to shock stresses from 0.3 to 170 GPa. Shock-induced deformation mechanisms are identified by examining the wave velocity and stress profiles as the shock wave propagates through the impactor.

DISCUSSION OF SIMULATION RESULTS

Shock-impact experiments[7] conducted on a number of different materials over a wide range of impact velocities have revealed the existence of a linear relationship between the shock-front velocity U_s and impact velocity U_p (i.e., the shock Hugoniot) in the absence of phase transformations.[8] Extrapolation of the linear U_s-U_p Hugoniot data to $U_p=0$ yields a shock-velocity–intercept value that is very close to the bulk sound speed c_b, which, in turn, is related to the longitudinal-wave speed c_l through the equation

$$c_b^2=c_l^2-\frac{4G}{3\rho}\ , \tag{6}$$

where G is the shear modulus and ρ is the mass density. With a knowledge of the bulk and longitudinal speeds, such extrapolation permits characterization of the shear modulus in the shocked material.

The experimental Hugoniot data[7] for copper in Fig. 1 follows a linear form with a U_s intercept of 3.91 km/sec, which is very close to the bulk sound speed value of 3.93 km/sec. From Eq. (6) we see that the shear modulus in the shocked material must be near zero for this to occur. In these samples, shear strength is lost even at very low impact velocities since their polycrystalline and defective nature allows plastic deformation to proceed in the absence of nucleation events.

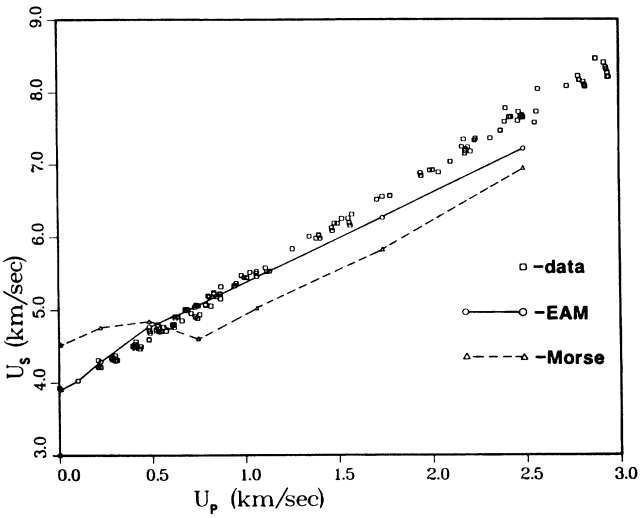

FIG. 1. Experimental and simulated shock Hugoniot plots. The experimental data are represented by the least-squares fit: $U_s=3.91+1.51U_p$.

An important distinction appears between the many-body and pairwise Hugoniot curves in Fig. 1. At large impact velocities ($U_p>0.7$ km/sec), U_s depends linearly on U_p in both cases. In the pairwise case, the U_s intercept is in reasonable agreement with the bulk sound velocity. This is expected for large impact velocities, which produce stresses much larger than the material shear strength. The many-body U_s intercept for this regime ($U_p>0.7$ km/sec), however, is near 4.2 km/sec, intermediate between c_b and the small-amplitude longitudinal-wave speed $c_l=4.76$ km/sec. This suggests that shear relaxation in the many-body copper at high U_p is not complete on the time scale of these simulations.

For impact velocities $U_p<0.7$ km/sec the many-body Hugoniot curve remains linear down to the smallest impact velocities studied, whereas the pairwise Hugoniot curve shows significant nonlinear behavior in this regime. The nonlinear behavior of the pairwise copper suggests that it possesses a significant shear modulus in this regime. The shock velocity at $U_p=0.01$ km/sec is 4.53 km/sec, in reasonable agreement with the expected value of 4.76 km/sec for small-amplitude longitudinal waves in copper. Thus, the shear modulus of the pairwise copper in this regime is nearly equal to that of the unshocked state. This result, which suggests that shear relaxation does not take place in this regime of impact velocity, is consistent with previous pairwise studies.[4]

In contrast, the intercept of the many-body Hugoniot curve is 3.90 km/sec, in agreement with the experimental bulk sound speed. These results infer that the many-body copper loses its shear strength at impact velocities as low as 0.01 km/sec (the slowest case considered), which is 2 orders of magnitude smaller than the corresponding velocity for the pairwise copper. This distinction reflects an

influence of the many-body interactions in the shock process.

Time-resolved lattice configurations from the two sets of simulations (Fig. 2) also reveal qualitative differences. In pairwise simulations up to $U_p = 0.22$ km/sec, the impactor experiences simple uniaxial strain [as illustrated in Fig. 2(a) for $U_p = 0.01$ km/sec], with no relaxation or lattice instability. At 0.48 km/sec [Fig. 2(b)], a region appears behind the shock front where the lattice planes buckle perpendicular to the shock direction. The lattice buckling is gradual, and reverses a small distance behind the shock front, so that the state of uniaxial strain is recovered. When the impact velocity is increased further [to 1.74 km/sec in Fig. 2(c) and 2.49 km/sec in Fig. 2(d)], permanent crystallographic damage appears in the simulations.

The behavior observed in the many-body simulations is quite different. Even at $U_p = 0.01$ km/sec [Fig. 2(e)], instead of a uniaxially strained cubic lattice, a twinning plane propagates behind the shock front. The generation of this twinning plane dramatically alters the many-body shock velocity, as exemplified by the Hugoniot plot in Fig. 1. Sumino[9] has demonstrated experimentally that the shear strength in the neighborhood of a twinning plane is a tiny fraction (perhaps 1%) of that displayed by a perfect crystal, due to the ability of twinning dislocations to move in response to applied shear stress. Hence, the reduction in shock velocity in the many-body copper is due to the formation of a twinning plane and the consequent loss of shear strength, which causes the velocity to approach the value of the bulk sound speed without any occurrence of permanent lattice damage. This result conflicts with the conventional view of shock-wave propagation, which assumes that shear strength is reduced only when plastic deformation occurs.

At moderate impact velocities [e.g., $U_p = 0.48$ km/sec in Fig. 2(f)] a martensitic region appears behind the shock front in the many-body simulations. In this region, which is about 1–2 nm in extent and is bounded by a pair of twinning planes, the symmetry of the lattice varies from a uniaxially strained fcc structure ahead of the martensitic region to a monoclinic structure within the region, reverting to uniaxial strain behind the martensitic region. At higher impact velocities, permanent crystallographic damage finally appears in the many-body simulations [Figs. 2(g) and 2(h)].

The distinction between the pairwise and many-body simulations is further illustrated in Fig. 3, where profiles of the shear stress components T_{yz} and T_{zx} are displayed for the case when $U_p = 0.48$ km/sec [corresponding to the lattice configurations in Figs. 2(b) and 2(f)]. Whereas the pairwise shear stress components vary gradually over the

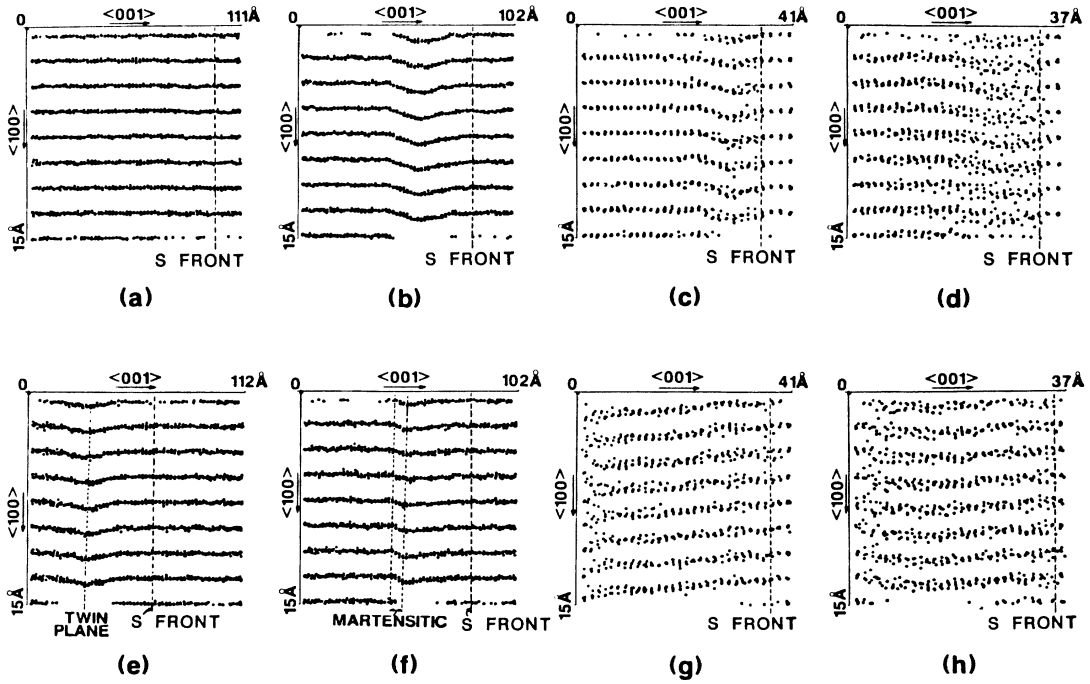

FIG. 2. Time-resolved lattice configurations as a function of impact velocity for the pairwise [(a)–(d)] and many-body [(e)–(h)] simulations. $U_p = 0.01$ km/sec for (a) and (e), $U_p = 0.48$ km/sec for (b) and (f), $U_p = 1.74$ km/sec for (c) and (g), and $U_p = 2.49$ km/sec for (d) and (h). S FRONT and the adjacent vertical dashed line denote the location of the shock front. Note the compressed scales in the ⟨001⟩ direction of ~100 Å as compared to the ⟨100⟩-direction scale of 15 Å.

buckled region of the impactor lattice [Figs. 3(a) and 3(b)], in the equivalent many-body simulation the component T_{yz} gradually decreases following the shock front, reaching a minimum at the leading edge of the martensitic region [Fig. 3(c)], while the T_{zx} component rises abruptly near the trailing edge of the martensitic region [Fig. 3(d)]. The strong correlation of the shear stress excursions with the twinning planes confirms that the structural aspects of shock loading in the pairwise and many-body simulations are not equivalent on a microscopic level.

Because of the magnitude of the thermal noise (excursions of several GPa on this size scale), the degree of shear relaxation at low impact velocities cannot be determined directly from maximum shear stress profiles. However, by considering the shock velocities at low-velocity impact and the shear stress profiles for high-velocity impact, it is possible to construct a consistent picture of shear relaxation in various regimes of shock loading. In the pairwise copper, there is no shear relaxation at impact velocities significantly below 0.5 km/sec. Above this value, there exists an intermediate region in

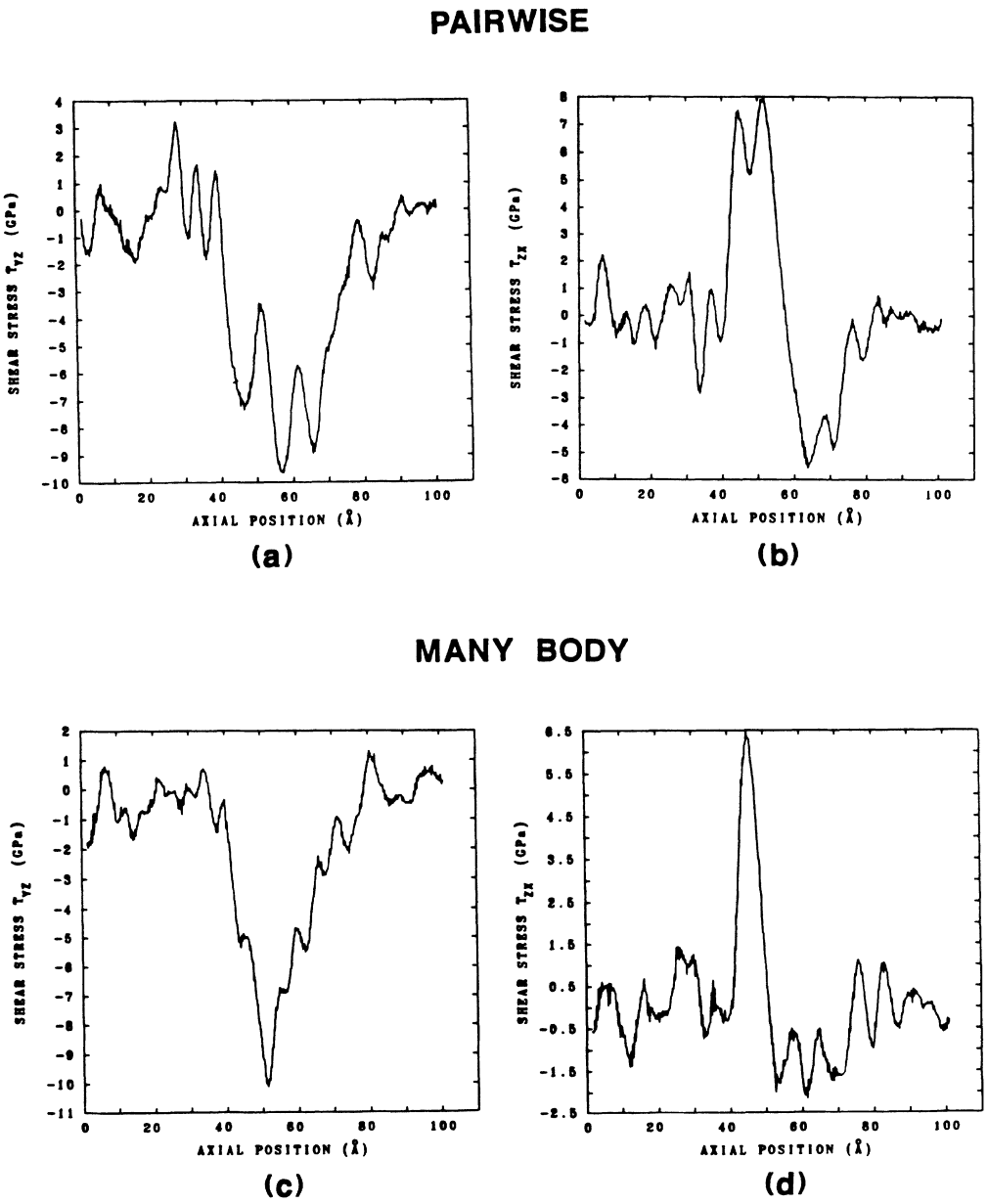

FIG. 3. Time-resolved shear stress profiles T_{yz} and T_{zx} for $U_p = 0.48$ km/sec: (a) and (b), pairwise copper; (c) and (d), many-body copper.

which a portion of the shear stress is relieved, with complete relaxation via plastic deformation occurring at $U_p \sim 1.0$ km/sec.

A completely different pattern is displayed by the many-body shock simulations. Low-velocity (0.01–0.7 km/sec) impacts show total shear stress relaxation, caused by formation of twinning planes. A kink in the Hugoniot curve near 0.5 km/sec indicates a crossover between two different deformation modes. At higher impact velocities only partial shear relaxation is observed on the simulated time scale, in agreement with the Hugoniot curve extrapolations described earlier. Plastic deformation thus appears to be much more difficult to initiate in the many-body copper than in the pairwise copper.

CONCLUSIONS

In summary, we have performed the first molecular dynamics shock-wave simulations which include a realistic many-body description of the atomic interactions. The key result centers on the appearance of structural instabilities at impact velocities 1–2 orders of magnitude lower than in the pairwise simulations. The twinning plane and martensitic region appearing in the many-body copper model are stable and localized nonlinear structures propagating at a constant velocity behind the shock front. Formation of these structures yields a major reduction in shock velocity without precipitating permanent lattice damage, contrary to the conventional view of shock loading.

The qualitative importance of many-body effects in shock loading suggests that such phenomena may also affect the shock-loading process in other classes of solids. In any case, the dramatic dependence of shock loading in copper on the details of atomic bonding shows that atomic-scale simulation of shock-wave propagation in solids must be treated as a materials-science problem. That is, the relevant details of metallic and chemical bonding must be included, in contrast to the traditional view that perceives the shock as a dramatic perturbation to the system in which chemical bonding has, at most, only a minor influence on the shock-loading process.

ACKNOWLEDGMENTS

We would like to thank B. L. Holian for useful and encouraging discussions. This work was performed at Sandia National Laboratories, which is operated for the U.S. Department of Energy under Contract No. DE-AC04-76DP00789.

[1]A. Paskin and G. J. Dienes, J. Appl. Phys. **43**, 1605 (1972); A. Paskin and A. Gohar, J. Phys. Chem. Solids **39**, 1307 (1978); A. Paskin, A. Gohar, and G. J. Dienes, J. Phys. C **10**, L563 (1977).

[2]D. H. Tsai and R. A. MacDonald, High Temp.-High Pressures **8**, 403 (1976); D. H. Tsai and R. A. MacDonald, J. Phys. C **11**, L365 (1978).

[3]V. Yu. Klimenko and A. N. Dremin, Dokl. Akad. Nauk SSSR **251**, 1379 (1980) [Sov. Phys.—Dokl. **25**, 288 (1980)].

[4]B. L. Holian, Phys. Rev. A **37**, 2562 (1988).

[5]S. M. Foiles, M. I. Baskes, and M. S. Daw, Phys. Rev. B **33**, 7983 (1986).

[6]G. C. Abell, Phys. Rev. B **31**, 6184 (1984).

[7]*LASL Shock Hugoniot Data,* edited by S. P. March (University of California Press, Berkeley, 1980).

[8]Ya. B. Zel'dovich and Yu. P. Raizer, *Physics of Shock Waves and High-Temperature Hydrodynamic Phenomena* (Academic, New York, 1966), Vol. I, pp. 45ff.

[9]K. Sumino, Phys. Status Solidi **33**, 327 (1969).